Available online at www.sciencedirect.com
SCIENCE DIRECT®
PERGAMON
Polyhedron 22 (2003) 293–297
POLYHEDRON
www.elsevier.com/locate/poly

The important role of an unpaired d-electron for terminal oxygen atom transfer reaction of the (hydroperoxo) iron(III) compound

Yuzo Nishida *, Sayo Ito, Satoshi Nishino

Department of Chemistry, Faculty of Science, Yamagata University, Yamagata 990-8560, Japan

Received 20 June 2002; accepted 14 October 2002

Abstract

Density–functional theory (DFT) calculations on the (hydroperoxo)–Fe(III) compound have revealed that a high-spin state of the iron(III) ion is essentially important for facile terminal oxygen atom transfer of the hydroperoxide ion to an organic substrate associated with heterolytic O–O bond cleavage. The validity of this concept is supported by several experimental results and this will give valuable information to elucidate the chemical mechanism of heme-oxygenase.

Keywords: Hydroperoxo-iron(III) species; Oxygen atom transfer reaction; Spin-state of iron(III) ion; Heme-oxygenase

1. Introduction

It is well known that a (hydroperoxo)metal species, M–OOH plays an important role in many biological oxygenases [1–4]. Very recently we have reported the electronic properties and reactivity of the (hydroperoxo)–metal species in terms of DFT calculated results [5,6] and pointed out that the reactivity of the M–OOH species is highly dependent on the structural properties of an intermediate containing a (hydroperoxo)–metal species, and also the electronic structure of a substrate, number of d-electrons and spin-state of a metal ion, etc. [5,6].

Since a (hydroperoxo)iron(III) species adduct has been assumed as an active species in the reaction course of heme-oxygenase (HO), [3] it is anticipated that the spin-state of an iron(III) ion in the active species should give a notable effect on the reaction of HO (see the figure below), however, such discussion has never been developed until now. In this study we have investigated the effect of spin-state of an iron(III) ion on the terminal oxygen atom transfer reaction of Fe(III)–OOH on the basis of density–functional theory (DFT) calculations; in the case of the high-spin state, the situation corresponds to **Case-A**, and in the low-spin state, to **Case-B**.

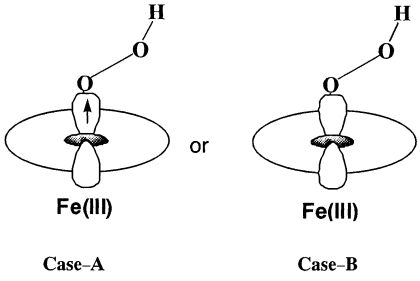

2. DFT calculations and its application to elucidation of reaction mechanism of heme-oxygenase

The DFT [7] calculations were done by using two ways: (I) DGAUSS 4.1 from Oxford Molecular Science, Oxford (1998); basis set, DZVP; gradient GGA X B88, GGA C LYP88 [8,9]. (II) Q-CHEM from Q-Chem. Inc., Pittsburgh (1998). Basis set, 3-21G; hybrid LYP; unrestricted hybrid HF-DFT SCF calculations were performed using Pulay DIIS extrapolation: exchange 0.20 Hartree–Fock +0.080 Slater +0.720 Becke; correlation: 0.8100 GGA91 +0.1900 Perdew–Zunger [7]. DGAUSS 4.1 was performed for the iron(III) complex with octamethyl-porphyrin (OM-por), Fe(OM-por)(O-

* Corresponding author. Fax: +81-23-628-4591
E-mail address: yuzo@sci.kj.yamagata-u.ac.jp (Y. Nishida).

0277-5387/02/$ - see front matter
PII: S0277-5387(02)01362-1

H_2)(OOH), [10] and Q-CHEM was applied for the iron(III) complex with tetramethyl-2,2′-dipyrromethene (DP), Fe(DP)$(H_2O)_3$(OOH) (see below) because of the limitation of the computer capacity. All the calculations were performed for Fe(DP)$(H_2O)_3$(OOH) with a torsion angle O2–O1–Fe–N (ligand DP) = 45°, α (angle Fe–O1–O2) = 100°–120° and β (angle O2–O1–H) = 120–230° (see the figure below). Thus, the C* atom is present almost in the Fe–O1–O2–H plane.

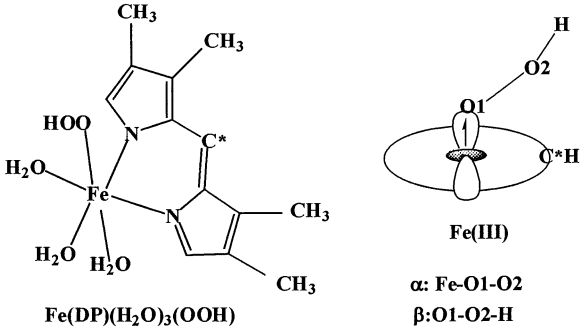

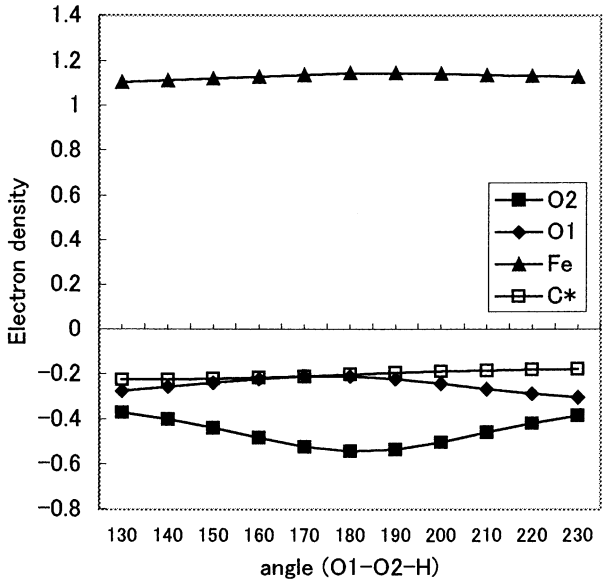

Fig. 2. Change of electron density (Mulliken net atomic charges) at the atoms in Fe(DP)$(H_2O)_3$(OOH); $\alpha = 110$. (Low-spin state; Q-CHEM.)

2.1. Calculated results

Fig. 1 shows the change of electron density (Mulliken net atomic charges) at the oxygen atoms of the peroxide ion in Fe(OM-por)(OH_2)(OOH); H_2(OM-por) denotes octamethyl-porphyrin, and in these cases the torsion angle (O2–O1–Fe–N(porphyrin)) was fixed at 45° throughout the calculations [10]. As reported earlier, the electron density at the oxygen atoms is highly dependent on the angle β (=O1–O2–H), but its change is continuous when the iron(III) complex is of low-spin state. Similar results were observed for the iron(III) complex with (DP), Fe(DP)$(H_2O)_3$(OOH) of low-spin state (Fig. 2). It should be noted here that the change of electron density at the oxygen atoms in the case of high-spin species is quite different from those obtained for the low-spin state, as illustrated in Figs. 3 and 4 (the calculation did not converge when the DGAUSS 4.1 was applied to the high-spin state of Fe(OM-por)(O-H_2)(OOH) where β is in the range 150°–200°, which may be due to the occurrence of an interaction between the hydroperoxy ion and porphyrin ring). The change is not continuous and this discontinuity is always accompanied by the discontinuity in electron density at the iron ion and carbon atom (C* in the figure above) of the

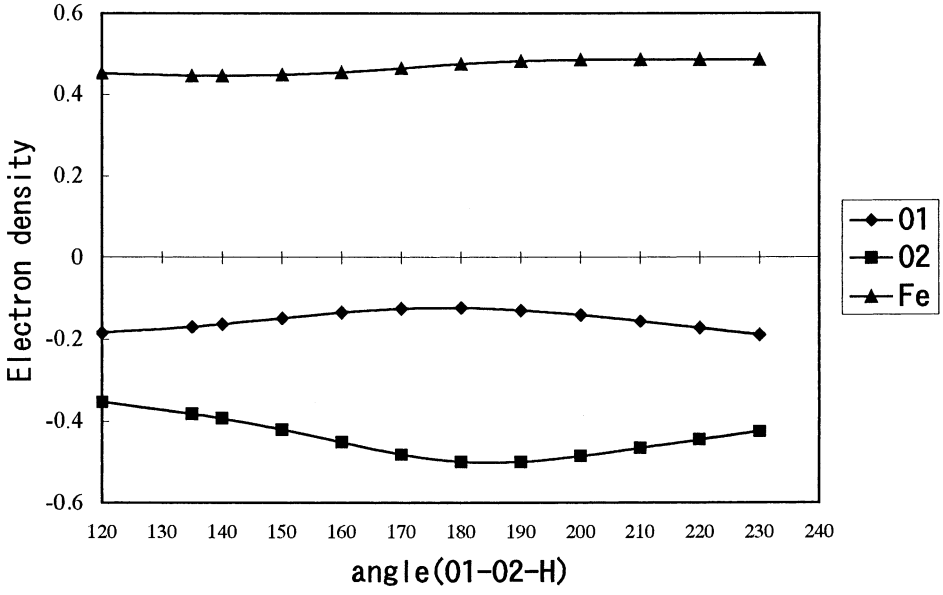

Fig. 1. Change of electron density (Mulliken net atomic charges) at the atoms in Fe(OM-por)(OH_2)(OOH); $\alpha = 100$. (Low-spin state; DGAUSS 4.1.)

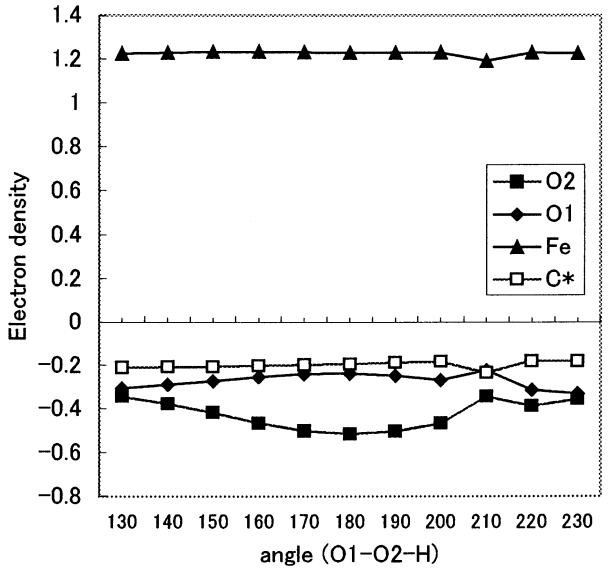

Fig. 3. Change of electron density (Mulliken net atomic charges) at the atoms in $Fe(DP)(H_2O)_3(OOH)$; $\alpha = 120$. (High-spin state;Q-CHEM.)

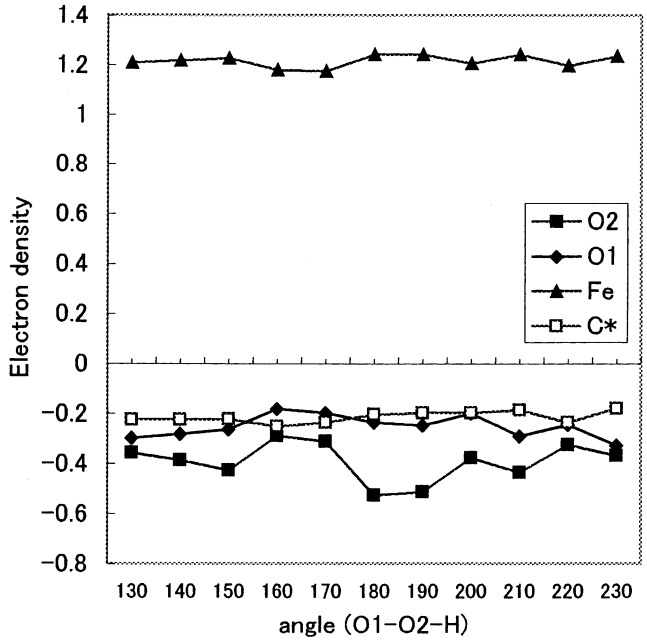

Fig. 4. Change of electron density (Mulliken net atomic charges) at the atoms in $Fe(DP)(H_2O)_3(OOH)$; $\alpha = 110$. (High-spin state;Q-CHEM.)

ligand system, which is the most adjacent to the O2 atom. The smaller the angle α (=Fe–O1–O2) is, the more drastic the discontinuity in change is (see Figs. 3 and 4). The remarkable change is the decrease of the electron density at the peroxide oxygen atoms, and increases at both the iron and carbon atoms. This behavior should correspond to O–O bond cleavage of the peroxide ion associated with the electron transfer from the peroxide ion to both the iron atom and carbon atom of the organic moiety (see the figure below). The present results also indicate that the position of the proton of the Fe(III)–OOH species is closely related with the reactivity of the peroxide adduct as proposed in our previous paper [5,6].

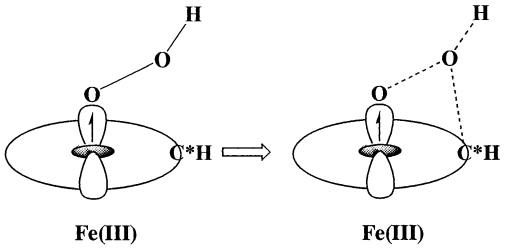

Above results suggests that heterolytic O–O bond cleavage of the peroxide ion is dependent on the spin state of the Fe(III) ion, and this seems to be consistent with our previous discussion on the DNA cleavage reaction catalyzed by Fe(III)–bleomycin–(OOH) species [11]. The bleomycin (BLM) family of glycopeptide antibiotics is used in combination with chemtherapy against several types of cancers, [12] and it has been established that a double-strand DNA cleavage reaction is performed by the action of Fe(III)–(BLM)–(OOH) species, [13] whereas no oxygen activation of any kind has been noted with the kinetically inert low-spin cobalt(III) complexes with BLM, and cobalt(III)–BLM–(OOH) do not inflict damage on DNA under aerobic conditions [14]. However, it has been reported that Co(III)–BLM–(OOH) do cleave DNA when illuminated with UV or visible light, and this photoinduced DNA strand scission is insensitive to oxygen. We have proposed [11] a new idea to elucidate the above facts based on the electronic structure of the metal chelates; the most important point is that when the Co(III)–BLM–(OOH) is irradiated with 366 nm light, the excited state occurs, where one unpaired electron resides in the d_{x^2}-orbital which is interacting with the OOH group directly, and this state is very similar electronically to the high-spin state of Fe(III)–(BLM)–(OOH). In the low-spin state of both the Fe(III) and Co(III) species, the d_{x^2}-orbital is empty as illustrated in Fig. 5. Thus, the present calculated results are consistent with the above discussion, because double-strand DNA cleavage by high-spin Fe(III)–BLM–(OOH) has been

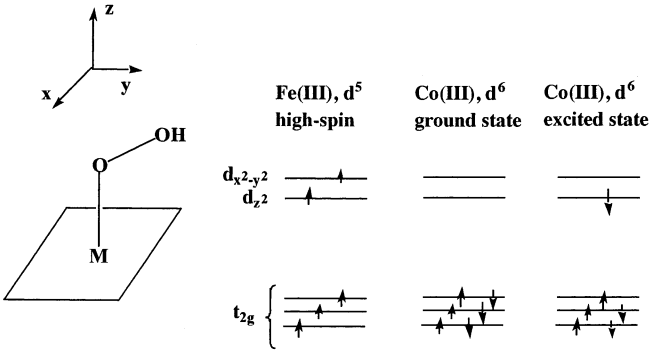

Fig. 5. Electronic configurations of Fe(III) and Co(III) compounds.

believed to proceed through the oxygenation of the sugar moiety of the DNA chain (see below).

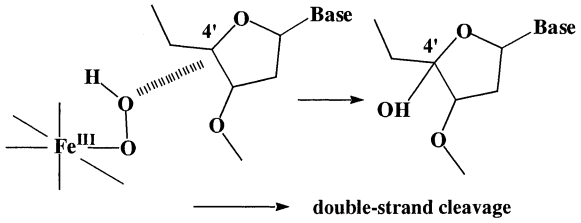

2.2. Reaction mechanism of heme-oxygenase

The degradation of heme by heme-oxygenase (HO) involves the formation of a heme-protein in which the heme-iron coordinates to a neutral imidazole of histidine, followed by three cycles of oxygenation in which the heme binds and activates O_2 [3]. The first monooxygenation step of HO catalysis is believed to convert the heme to α-*meso*-hydroxyheme, and it has been proposed to proceed by reduction of the O_2-bound complex to a hydroperoxy-ferric active intermediate, [3,4] rather than the oxy-ferryl state proposed to occur in P-450 [1]. Very recently, Davydov et al. [15] have succeeded in establishing that hydroperoxy-HO indeed catalyzes the formation of α-*meso*-hydroxyheme by the use of ESR and ENDOR techniques, and to show that it can do so in situ at temperatures above 200 K. They reported that the hydroperoxy-HO is of low-spin state under 200 K, but upon annealing the species to temperatures above 200 K its ESR spectrum disappeared, paralleled by a corresponding increase in that from high-spin ferricheme, and they concluded that this signal corresponds to that of high-spin α-*meso*-hydroxyheme. It should be noted here that the reaction of native HO enzyme proceeds at room temperature, but not at 77 K.

Present results may give a reasonable explanation on the ESR spectral change observed by Hoffman et al., especially for the loss of ESR signal of the low-spin state when the oxygenation reaction proceeds above 200 K; i.e. the high-spin state of the hydroperoxy-heme is essentially important for the oxygenation catalyzed by heme-oxygenase; the presence of the molecular orbital derived from a d-orbital containing one unpaired electron (in this case the d_{x^2}-orbital of Fe(III) ion) and the peroxide ion is necessary for facile cleavage of the O–O bond of the peroxide adduct to induce one oxygen atom transfer to the substrate, which is quite different from that of P-450 where the Fe(III) ion is of low-spin type, and thus there is no d-electron in the d_{x^2}-orbital. It is clear that the reactivity of the terminal oxygen atom of low-spin Fe(III)–(OOH) is different from that of the HO, one example which is characteristic for cytochrome P-450 (CYP17, 17α-hydroxylase-17,20-lyase) [2] is shown below.

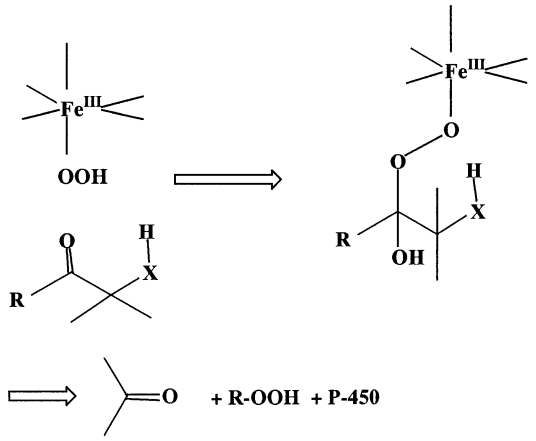

This should be due to the strong oxidative power of the low-spin Fe(III)–(OOH) species, which may be due to the fact that the vacant orbital composed of d_{x^2}-orbital and π*-orbital of peroxide ion exhibits reactivity similar to singlet oxygen ($^1\Delta_g$) [4].

3. DNA cleavage reaction and spin-state of cobalt ion in the active species

In this study we have investigated the DNA cleavage reaction by the dinuclear cobalt(II) complex with H(HPTP), [16] $Co_2(HPTP)Cl_2(ClO_4)_2$, and found that the reactivity of a peroxide adduct of Co(II) species towards DNA is quite different from that of the corresponding Co(III) species. This also supports the conclusion described above.

As shown in Fig. 6, the DNA cleavage patterns by the $Co_2(HPTP)Cl_2(ClO_4)_2$ complex are highly dependent on the reaction conditions. It is noteworthy that the presence of hydrogen peroxide highly affects the cleavage reaction (see lanes 5, 6, 7 and 8). As described in our previous paper, [16] the freshly prepared solution of cobalt(II) complex can cleave DNA facilely under an aerobic condition (see lane 4; single-strand scission). In contrast to this, 'the aged cobalt(II) complex solution', 10 days after the cobalt(II) complex was prepared, does not exhibits DNA cleavage ability (not shown). The absorption spectrum of the aged solution is similar to that of the solution containing $Co_2(HPTP)Cl_2(ClO_4)_2$ and hydrogen peroxide, and is completely different from that of the freshly prepared cobalt(II) complex solution. This suggests that the Co(II) ion of the original complex is gradually converted to a Co(III) ion by oxygen in solution, and binding of the cobalt(II) complex and oxygen is greatly accelerated by DNA [16]. These all support that an active species for single-strand DNA cleavage by the $Co_2(HPTP)Cl_2(ClO_4)_2$ complex, observed in lanes 4, 7 and 8, should be Co_2^{III} –(HPTP)–

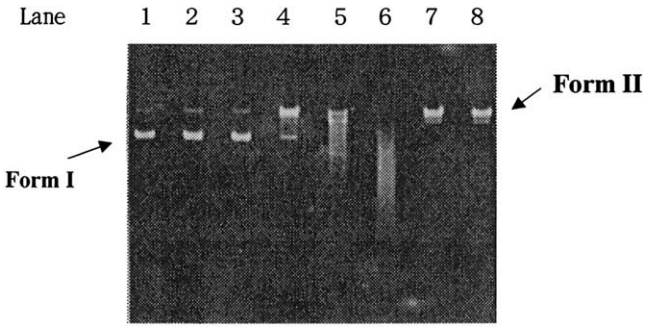

Fig. 6. Supercoiled ds-DNA (pBR322) was incubated with Co(II) complex. Lanes (1) DNA alone (2) DNA + H_2O_2 (1/100 M solution) (3) DNA + H_2O_2 (1/10 M solution) (4) DNA + freshly prepared Co(II) complex solution; (5) H_2O_2 (1/100 M solution) was added to the solution of DNA and freshly prepared Co(II) complex; (6) H_2O_2 (1/10 M solution) was added to the solution of DNA and freshly prepared Co(II) complex; (7) DNA was added to the solution containing Co(II) complex and H_2O_2 (1/100 M solution); (8) DNA was added to the solution containing Co(II) complex and H_2O_2 (1/10 M solution). In the case of lanes (7) and (8), the DNA was added 1 h after Co(II) complex was mixed with hydrogen peroxide solution.

O_2^{2-}. The difference in the cleavage pattern between lane 5 (or 6; double-strand scission) and lane 7 (or 8; single-strand scission) should be due to the difference of the oxidation state of the cobalt ion; i.e. in the former case, cobalt(II) is present in the system, on the other hand an active species for DNA cleavage should be Co(III)–OOH in the latter case. Since the complex Co_2^{II}(HPTP)$Cl_2(ClO_4)_2$ is of high-spin type, it is likely that the electronic structure of a cobalt(II)–OOH species, which is assumed to operate in lanes 5 and 6, should be similar to that of **Case-A** (high-spin Fe(III) species), and of the cobalt(III)–OOH in lanes 7 and 8 and also 4, to **Case-B** (low-spin Fe(III) species), because the d-orbitals which interact with hydrogen peroxide in the cobalt(III) compounds are all vacant.

4. Experimental

4.1. DNA cleavage by binuclear cobalt(II) compound

In a typical run, a freshly prepared aqueous solution of cobalt(II) complex, Co_2(HPTP)$(CH_3COO)(ClO_4)_2$ (4 μl, 1 mM), DNA (pBR322, 4 μl of 0.1 mg ml^{-1} solution) and tris buffer (2 μl of 0.1 M solution) were mixed in the absence or presence of H_2O_2 solution (1 μl of 0.1–0.01 M solution), and allowed to stand for 1 h. The resulting solution was electrophorated on 0.9% agarose gel containing ethidium (3,8-diamino-5-ethyl-6-phenylphenanthridimium) bromide. The bands were photographed with Polaroid 667 film [17].

5. Supplementary data

The details and results of DFT calculations will be available on request to Y.N. by air-mail.

References

[1] M. Sono, M.P. Roach, E.D. Coulter, J.H. Dawson, Chem. Rev. 96 (1996) 2841.
[2] D.L. Wertz, J.S. Valentine, Structure and Bonding, vol. 97 (Chapter 2), Springer, Berlin, 2000.
[3] P.R.O. Montellano, Acc. Chem. Res. 31 (1998) 543.
[4] Y. Nishida, Trends Inorg. Chem. 3 (1998) 89.
[5] S. Nishino, T. Kobayashi, H. Matsushima, T. Tokii, Y. Nishida, Z. Naturforsch., Teil. C 56 (2001) 138.
[6] Y. Nishida, S. Nishino, Z. Naturforsch., Teil C 56 (2001) 144.
[7] R.G. Parr, W. Yang, Density–Functional Theory of Atoms and Molecules, Oxford University Press, London, 1989.
[8] A.D. Becke, Phys. Rev. A38 (1988) 3098.
[9] C. Lee, W. Yang, R.G. Parr, Phys. Rev. B37 (1988) 785.
[10] Y. Nishida, Inorg. Chem. Commun. 3 (2000) 310.
[11] Y. Nishida, M. Kunita, S. Nishino, Inorg. Chem. Commun. 2 (1999) 156.
[12] J. Stubbe, J.W. Kozarich, Chem. Rev. 87 (1987) 1107.
[13] J.W. Sam, X.-J. Tang, J. Peisach, J. Am. Chem. Soc. 116 (1994) 5250.
[14] W. Wu, D.E. Vanderwal, C.J. Turner, J.W. Kozarich, J. Stubbe, J. Am. Chem. Soc. 118 (1996) 1281.
[15] R.M. Davydov, T. Yoshida, M. Saito, B.M. Hoffman, J. Am. Chem. Soc. 121 (1999) 10656.
[16] Y. Nishida, S. Nishino, L.L. Guo, M. Kunita, H. Matsushima, T. Tokii, Inorg. Chem. Commun. 2 (1999) 609.
[17] D.A. Micklos, G.A. Freyer, DNA Science, Cold Spring Harbour Laboratory Press, New York, 1990.